Robust three-qubit search algorithm in Rydberg atoms via geometric control

Bing-Bing Liu,[1] Zheng Shan,[2,*] M.-R. Yun,[1] D.-Y. Wang,[1] B.-J. Liu,[3,†] L.-L. Yan,[1,‡] M. Feng,[4,5,6] and S.-L. Su[1,§]

[1]*Key Laboratory of Material Physics, Ministry of Education, School of Physics and Microelectronics, Zhengzhou University, Zhengzhou 450001, China*

[2]*State Key Laboratory of Mathematical Engineering and Advanced Computing, Zhengzhou 450001, Henan, China*

[3]*Department of Physics, Southern University of Science and Technology, Shenzhen, Guangdong 518055, China*

[4]*State Key Laboratory of Magnetic Resonance and Atomic and Molecular Physics, Wuhan Institute of Physics and Mathematics, Innovation Academy of Precision Measurement Science and Technology, Chinese Academy of Sciences, Wuhan 430071, China*

[5]*Research Center for Quantum Precision Measurement, Guangzhou Institute of Industry Technology, Guangzhou 511458, China*

[6]*Department of Physics, Zhejiang Normal University, Jinhua 321004, China*

(Received 3 June 2022; accepted 14 November 2022; published 28 November 2022)

Rydberg atoms possess long coherence time and inherent scalability, which makes it promising to implement quantum algorithms. An exact and robust quantum search algorithm (SA) is essential to some practical applications. Here we propose a multisolution three-qubit SA by employing quantum circuit and geometric operations, in which the target states can be successfully searched with the fidelity of at least 99.8% and the geometric operators guarantee robustness against systematic errors. In particular, the geometric three-qubit gate operators employed reduce the implementation time and help to resist against the detrimental influence of decoherence. Moreover, our scheme can be straightforwardly extended to multiqubit cases. We have carried out numerical simulations based on the master equation to illustrate the superiority of our scheme. We consider that our study provides an alternative method for executing quantum SAs with high success probability.

DOI: 10.1103/PhysRevA.106.052610

I. INTRODUCTION

Rydberg atoms possess a relatively long coherence time and inherent scalability, which makes them a promising platform for quantum information processing [1]. When excited to high-lying Rydberg states, the neutral atoms exhibit strong, long-range, and controllable Rydberg-Rydberg interactions [1,2], leading to Rydberg blockade [3–12] and antiblockade [13–18] associated with many potential applications, such as quantum computation [19–22], entangled state preparation [5,23], and quantum simulators [24–26]. Recent studies have demonstrated the advantage of studying quantum algorithms in Rydberg atoms. For example, with Rydberg atom arrays, Ebadi *et al.* [27] executed experimentally the quantum algorithm for solving the maximum independent set problem, Graham *et al.* [28] achieved the quantum phase estimation algorithm and the quantum approximate optimization algorithm, and Dlaska *et al.* [29] proposed a scheme to implement the quantum approximate optimization algorithm for small-scale test problems via a four-body Rydberg parity gate.

Quantum computation can solve some problems exponentially faster than its classical counterpart [30,31]. Taking Grover's algorithm as an example, which aims to search in an unsorted database with N elements, we may accomplish the search with $O(\sqrt{N})$ steps, quadratically faster than the classical search algorithm [32–39]. There have been some experimental reports for executing the Grover search using different physical systems, such as nuclear magnetic resonance [40], cavity quantum electrodynamics [41–43], trapped ions [44–47], and optical system [48]. For the original Grover's algorithm, however, the successful probability of searching the targeted state is not exactly of unity. In practice, the certainty for the search result is very important for some problems, e.g., quantum pattern recognition [49] and divide-and-verify strategy [50]. Although there have been some quantum circuits (QCs) used to realize a quantum search algorithm with high success probability, how to search a multisolution multiqubit target state with a high success probability is still challenging.

Systematic errors arising from inaccurate control of parameters inevitably affect the implementation efficiency of quantum operations. Geometric quantum computation has been proposed to realize high-fidelity quantum manipulation, which is robust to control errors due to the intrinsic characteristics of the geometric phases [51–57]. Early geometric quantum computation was executed in an adiabatic fashion, e.g., the adiabatic holonomic quantum computation based on Abelian and non-Abelian geometric phases [58–60]. Now geometric quantum computation can be carried out nonadiabatically [61–64], which helps to reduce the detrimental influence of decoherence. Many geometric control schemes have been put forward to improve the efficiency of quantum operations [65–83].

*zzzhengming@163.com

†Present address: Department of Physics, University of Massachusetts–Amherst, Amherst, MA 01003, USA.

‡llyan@zzu.edu.cn

§Corresponding auther: slsu@zzu.edu.cn

In this work, we propose a scheme to exactly realize a multisolution three-qubit quantum search algorithm (SA) using QCs, in particular with Rydberg atoms via the geometric control method. Our scheme has the following favorable features: (i) In contrast to the previous QCs, the implementation process of our scheme is simpler because the complex design of quantum logic operations in QCs is avoided. (ii) Our scheme is robust to decoherence since the total evolution time is reduced. (iii) Our scheme is robust to systematic errors due to geometric quantum operations involved. (iv) Our scheme can be straightforwardly extended to realize multisolution multiqubit SAs. In addition, our research has implications for implementing other quantum algorithms using Rydberg atoms and other quantum platforms.

The outline of this paper is as follows. In Sec. II, the improved three-qubit SA based on QCs is illustrated. In Sec. III, we show how to realize a three-qubit SA via geometric control. Numerical simulation results are given to verify the robustness against decoherence and control errors in Sec. IV. Finally, Sec. V presents the conclusion and outlook.

II. IMPROVED THREE-QUBIT SA

In this section, we first talk about the basic theory used for exactly realizing one- and multisolution quantum SAs, and then we design the relevant QCs.

A. Basic theory

For the N-item ($N = 2^n$, where n is the number of qubits) search problem, we prepare the system initially in the uniform superposition state,

$$\begin{aligned}|\Psi_0\rangle = U^{\otimes n}|s\rangle &= \frac{1}{\sqrt{N}}\sum_{x=0}^{N-1}|x\rangle \\ &= \sqrt{\frac{M}{N}}|\alpha\rangle + \sqrt{\frac{N-M}{N}}|\chi\rangle \\ &= s_\beta|\alpha\rangle + c_\beta|\chi\rangle, \end{aligned} \tag{1}$$

where $|s\rangle = |1\rangle^{\otimes n}$ is the product state for the n-qubit system with $s_x = \sin x$ and $c_x = \cos x$, U is the Hadamard-like operator, M is the number of the target items, $|\alpha\rangle = 1/\sqrt{M}\sum_t |t\rangle$, and $|\chi\rangle = 1/\sqrt{N-M}\sum_{l\neq t}|l\rangle$, in which $|t\rangle$ represents target items and $|l\rangle$ represents nontarget items.

One cannot search the target items for certainty using the original Grover's algorithm, where the phase operators in a quantum oracle and diffusion are based on the phase inversion. Here we replace the phase inversion of the oracle and the diffusion operators by phase rotations: $P_\phi(|t\rangle) = I - (1-e^{i\phi})|t\rangle\langle t|$ and $R_\eta(|s\rangle) = I - U(1-e^{i\eta})|s\rangle\langle s|U^\dagger$, and the Grover transformation can be expressed as $G = -R_\eta(|s\rangle)P_\phi(|t\rangle)$. For our purpose, we set $\eta = \phi$ [84–87]. After one iteration of the Grover transformation $|\Psi_1\rangle = G|\Psi_0\rangle$, the successful probability is

$$P = s_\beta^2 c_\beta^4(5-4c_\phi) - 2c_\beta^2(-2c_\phi + c_{2\phi})s_\beta^4 + s_\beta^6. \tag{2}$$

The relationship among P, M/N, and ϕ is shown in Fig. 1. We see that, for a one-solution three-qubit SA ($M = 1$, $N = 8$), we cannot search the target state for certainty with one iteration of the Grover transformation no matter how large the phase value ϕ is. But we can search two- and multisolution target states ($M \geqslant 2$) with definite success probability using the iteration of the Grover transformation.

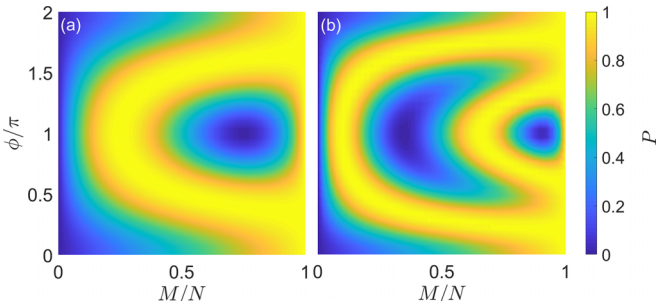

FIG. 1. Probability P as functions of M/N and ϕ for a quantum SA with one iteration (a) and two iterations (b) of the Grover transformation, where M is the number of targets and $N = 2^n$, with n the number of qubits.

To exactly realize the one-solution three-qubit SA, we implement the Grover transformation again, i.e., $|\Psi_2\rangle = G|\Psi_1\rangle$, with the successful probability

$$\begin{aligned} P = {} & [2(-1+4e^{-3i\phi}+5e^{-4i\phi})s_\beta + (-1+e^{-i\phi})^4 \\ & \times s_{5\beta} + 8e^{-2i\phi}s_{3\beta}s_{\phi/2}^2(3+3c_\phi - 2is_\phi)] \\ & \times [2(-1+4e^{3i\phi}+5e^{4i\phi})s_\beta + (-1+e^{i\phi})^4 s_{5\beta} + 8e^{2i\phi}s_{3\beta} \\ & \times s_{\phi/2}^2(3+3c_\phi+2is_\phi)]/256. \end{aligned} \tag{3}$$

The variation of the successful probability P with M/N and ϕ is presented in Fig. 1(b), from which we find that for the three-qubit SA, the one-solution target state can be searched exactly with an appropriate phase value ϕ after two iterations of the Grover transformation. From Fig. 1, we also find more than one value of ϕ for searching the target state, which may be useful for executing a quantum SA experimentally. Besides, we have no restriction on M and N, thus for a multisolution multiqubit SA, there may exist several phase values that can be used to exactly realize it within two iterations. Otherwise, we have to increase the number of iterations. Table I presents the specific implementation of three-qubit SAs.

B. QC design for a one-solution three-qubit SA

According to Sec. II A, we design the QC to exactly search a one-solution target state, as shown in Fig. 2 [88–90], including the following three steps.

TABLE I. The number of iterations, i.e., W, of the Grover transformation and the value of ϕ used for exactly searching one- and multisolution three-qubit SAs, where M is the number of the target.

M	1	2	3	4	5	6	7
W	2	1	1	1	1	1	1
$\frac{\phi}{\pi}$	0.677	1	0.608	0.498	0.436	0.392	0.361
	1.323		1.392	1.502	1.564	1.608	1.639

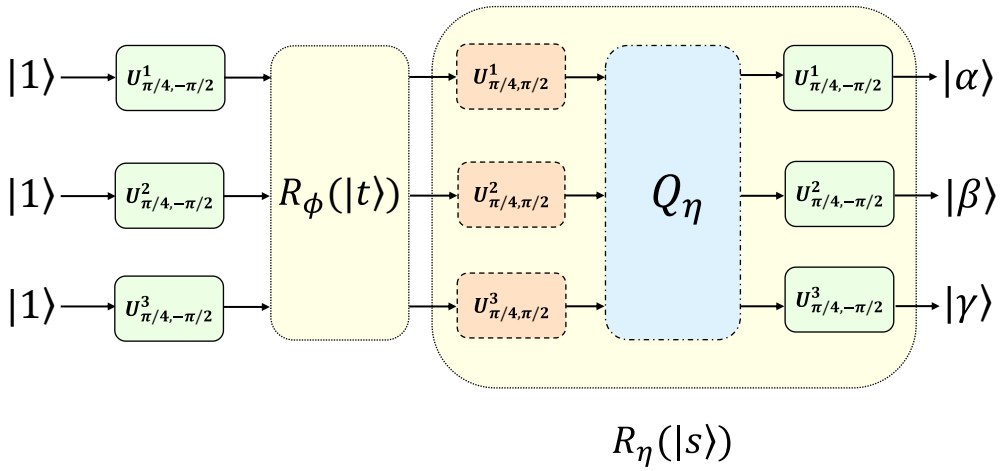

FIG. 2. QC for one- and multisolution three-qubit SAs, in which the operators $P_\phi(|t\rangle)$ and Q_η are accomplished by three-qubit gate operators, instead of a series of single- and two-qubit gate operators.

(i) Operator $U^k_{\pi/4,-\pi/2}$ is applied to each qubit with the initial state of $|1\rangle$, where

$$U^k_{\theta,\varphi} = \begin{pmatrix} c_\theta & -is_\theta e^{-i\varphi} \\ -is_\theta e^{i\varphi} & c_\theta \end{pmatrix}, \tag{4}$$

with respect to the basis spanned as $\{|0\rangle, |1\rangle\}$, and the superscript k denotes the operator acting on the kth atom. $U^k_{\pi/4,-\pi/2}$ rotates the qubit from $|1\rangle$ to $1/\sqrt{2}(|0\rangle + |1\rangle)$, resulting in the state

$$|\Psi_0\rangle = \frac{1}{2\sqrt{2}}(|000\rangle + |001\rangle + |010\rangle + |011\rangle + |100\rangle + |101\rangle + |110\rangle + |111\rangle). \tag{5}$$

(ii) Perform the operator $P_\phi(|t\rangle)$, in which $\phi = 1.323\pi$ for a one-solution SA according to II A, $|t_o\rangle$ represents the one-solution target state, and we use the subscript j ($j \in [1, 8]$) to distinguish different target states, i.e., $|t_{oj}\rangle$. We have $P_{1.323\pi}(|t_o\rangle) = I - (1 - e^{i1.323\pi})|t_o\rangle\langle t_o|$ for rotating the phase of the target state. If $|t_{o1}\rangle = |000\rangle$, then

$$P_{1.323\pi}(|t_{o1}\rangle) = \begin{pmatrix} e^{i1.323\pi} & 0 & 0 & 0 & 0 & 0 & 0 & 0 \\ 0 & 1 & 0 & 0 & 0 & 0 & 0 & 0 \\ 0 & 0 & 1 & 0 & 0 & 0 & 0 & 0 \\ 0 & 0 & 0 & 1 & 0 & 0 & 0 & 0 \\ 0 & 0 & 0 & 0 & 1 & 0 & 0 & 0 \\ 0 & 0 & 0 & 0 & 0 & 1 & 0 & 0 \\ 0 & 0 & 0 & 0 & 0 & 0 & 1 & 0 \\ 0 & 0 & 0 & 0 & 0 & 0 & 0 & 1 \end{pmatrix}. \tag{6}$$

If $|t_{o2}\rangle = |001\rangle$, we have

$$P_{1.323\pi}(|t_{o2}\rangle) = \begin{pmatrix} 1 & 0 & 0 & 0 & 0 & 0 & 0 & 0 \\ 0 & e^{i1.323\pi} & 0 & 0 & 0 & 0 & 0 & 0 \\ 0 & 0 & 1 & 0 & 0 & 0 & 0 & 0 \\ 0 & 0 & 0 & 1 & 0 & 0 & 0 & 0 \\ 0 & 0 & 0 & 0 & 1 & 0 & 0 & 0 \\ 0 & 0 & 0 & 0 & 0 & 1 & 0 & 0 \\ 0 & 0 & 0 & 0 & 0 & 0 & 1 & 0 \\ 0 & 0 & 0 & 0 & 0 & 0 & 0 & 1 \end{pmatrix}. \tag{7}$$

Other oracle operators $P_{1.323\pi}(|t_{oj}\rangle)$ used to search the remaining one-solution target states are similar to those above. We have noticed other three-qubit gates realized in experiments [4], which guarantees the feasibility of our above-proposed gate operators.

(iii) Perform the operator $R_\eta(|s\rangle) = I - U(1 - e^{i\eta})|s\rangle\langle s|U^\dagger$, which is realized by

$$R_\eta(|s\rangle) = U^1_{\pi/4,-\pi/2}U^2_{\pi/4,-\pi/2}U^3_{\pi/4,-\pi/2}Q_\eta \times U^1_{\pi/4,\pi/2}U^2_{\pi/4,\pi/2}U^3_{\pi/4,\pi/2}, \tag{8}$$

where

$$Q_\eta = \begin{pmatrix} 1 & 0 & 0 & 0 & 0 & 0 & 0 & 0 \\ 0 & 1 & 0 & 0 & 0 & 0 & 0 & 0 \\ 0 & 0 & 1 & 0 & 0 & 0 & 0 & 0 \\ 0 & 0 & 0 & 1 & 0 & 0 & 0 & 0 \\ 0 & 0 & 0 & 0 & 1 & 0 & 0 & 0 \\ 0 & 0 & 0 & 0 & 0 & 1 & 0 & 0 \\ 0 & 0 & 0 & 0 & 0 & 0 & 1 & 0 \\ 0 & 0 & 0 & 0 & 0 & 0 & 0 & e^{i\eta} \end{pmatrix} \tag{9}$$

in the one-solution three-qubit SA, and we set the phase value $\eta = \phi = 1.323\pi$.

Finally, we successfully search our desired one-solution target state with certainty when $G = -R_{1.323\pi}(|s\rangle)P_{1.323\pi}(|t\rangle)$ is applied twice to the initial state according to Sec. II A. In a previous scheme of the quantum SA, the operators $P_\phi(|t_o\rangle)$ and Q_η were realized by combining different single-qubit and three-qubit gate operators [88–91], which implies lengthy gate time and thus is more sensitive to decoherence. In contrast, the operators $P_\phi(|t_o\rangle)$ and Q_η employed here can be accomplished directly, and thus for a faster performance. In addition, our scheme can search the target states with definite success probability.

C. QC design for two- and multisolution three-qubit SAs

For a two-solution three-qubit SA, we can exactly search the target state by choosing the phase value $\phi = \pi$ and implementing the Grover transformation only once according to Sec. II A. The difference in the QC between two-solution and one-solution SAs is that we need to verify the phase rotation

operator $P_{1.323\pi}(|t_o\rangle)$ to flip the sign of the two-solution target state $P_\pi(|t_t\rangle)$, where $|t_t\rangle$ represents the two-solution target state, and we use the subscript f ($f \in [1, 28]$) to distinguish different target states, i.e., $|t_{tf}\rangle$. Supposing $|t_{t1}\rangle = 1/\sqrt{2}(|000\rangle + |001\rangle)$, we have

$$P_\pi(|t_{t1}\rangle) = \begin{pmatrix} e^{i\pi} & 0 & 0 & 0 & 0 & 0 & 0 & 0 \\ 0 & e^{i\pi} & 0 & 0 & 0 & 0 & 0 & 0 \\ 0 & 0 & 1 & 0 & 0 & 0 & 0 & 0 \\ 0 & 0 & 0 & 1 & 0 & 0 & 0 & 0 \\ 0 & 0 & 0 & 0 & 1 & 0 & 0 & 0 \\ 0 & 0 & 0 & 0 & 0 & 1 & 0 & 0 \\ 0 & 0 & 0 & 0 & 0 & 0 & 1 & 0 \\ 0 & 0 & 0 & 0 & 0 & 0 & 0 & 1 \end{pmatrix}. \quad (10)$$

If $|t_{t2}\rangle = 1/\sqrt{2}(|000\rangle + |010\rangle)$, then

$$P_\pi(|t_{t2}\rangle) = \begin{pmatrix} e^{i\pi} & 0 & 0 & 0 & 0 & 0 & 0 & 0 \\ 0 & 1 & 0 & 0 & 0 & 0 & 0 & 0 \\ 0 & 0 & e^{i\pi} & 0 & 0 & 0 & 0 & 0 \\ 0 & 0 & 0 & 1 & 0 & 0 & 0 & 0 \\ 0 & 0 & 0 & 0 & 1 & 0 & 0 & 0 \\ 0 & 0 & 0 & 0 & 0 & 1 & 0 & 0 \\ 0 & 0 & 0 & 0 & 0 & 0 & 1 & 0 \\ 0 & 0 & 0 & 0 & 0 & 0 & 0 & 1 \end{pmatrix}. \quad (11)$$

Other oracle operators $P_\pi(|t_{tf}\rangle)$ used to search the remaining two-solution target states are similar to the above operators. In our scheme, the operator $P_\pi(|t_t\rangle)$ can be achieved by combining two three-qubit controlled-phase gates, and these gate operators can be easily obtained. Compared with Ref. [91], in which the operator $P_\pi(|t_t\rangle)$ is realized by a series of single- and two-qubit gates, our scheme improves the efficiency of the two-solution three-qubit SA and exactly searches the two-solution target state.

A multisolution three-qubit SA can be exactly realized when choosing the approximate phase value and appropriate number of iterations of the Grover transformation. For different target states, the operator $P_\phi(|t\rangle)$ can also be easily obtained in our scheme, similar to cases of one- and two-solution quantum SAs mentioned above. The advantage of our scheme is that the operator $P_\phi(|t\rangle)$ is directly constructed by three-qubit gates without the combination of a series of single- and two-qubit gates, and the target states can be searched exactly. This allows us to implement the multisolution three-qubit SA more simply.

III. IMPLEMENTATION OF THE THREE-QUBIT SA

In this section, we first illustrate how to realize the universal single-qubit gates via geometric control, and then we expand to directly achieve multiqubit controlled-phase gates without resorting to a series of single- and two-qubit gate operators. Then we demonstrate how to exactly realize one- and multisolution three-qubit SAs via geometric control.

A. Geometric single- and multiqubit gates

Considering a quantum system consisting of three levels $\{|0\rangle, |1\rangle, |r\rangle\}$, we drive the transition $|0\rangle \to |r\rangle$ ($|1\rangle \to |r\rangle$) using a resonant control field with the Rabi frequency $\Omega_0(t)e^{i\phi_0(t)}$ ($\Omega_1(t)e^{i\phi_1(t)}$). Under the rotating-wave approximation, the Hamiltonian in the interaction picture can be written as $H(t) = \sum_{i=0}^{1}[\frac{\Omega_i(t)}{2}e^{i\phi_i(t)}|i\rangle\langle r| + \text{H.c.}]$. Defining a bright state $|b\rangle = -s_{\frac{\theta}{2}}e^{-i\phi}|0\rangle + c_{\frac{\theta}{2}}|1\rangle$, in which $\tan\frac{\theta}{2} = \Omega_0(t)/\Omega_1(t)$ and $\phi = \phi_1(t) - \phi_0(t) - \pi$, we keep θ and ϕ time-independent, and thus state $|b\rangle$ is time-independent, too. Then the Hamiltonian can be rewritten as $H(t) = \frac{\Omega(t)}{2}e^{i\phi_1(t)}|b\rangle\langle r| + \text{H.c.}$, with $\Omega(t) = \sqrt{\Omega_0(t)^2 + \Omega_1(t)^2}$. Parameters of the Hamiltonian used to construct universal gate operators are chosen as [79]

$$\begin{aligned}
&\int_0^{\frac{\tau}{8}} \Omega(t)dt = \pi/2, \quad \phi_1 = 0, \quad t \in [0, \tau/8], \\
&\int_{\frac{\tau}{8}}^{\frac{3\tau}{8}} \Omega(t)dt = \pi, \quad \phi_1 = -\pi/2, \quad t \in (\tau/8, 3\tau/8], \\
&\int_{\frac{3\tau}{8}}^{\frac{\tau}{2}} \Omega(t)dt = \pi/2, \quad \phi_1 = 0, \quad t \in (3\tau/8, \tau/2], \\
&\int_{\frac{\tau}{2}}^{\frac{5\tau}{8}} \Omega(t)dt = \pi/2, \quad \phi_1 = \gamma + \pi, \quad t \in (\tau/2, 5\tau/8], \\
&\int_{\frac{5\tau}{8}}^{\frac{7\tau}{8}} \Omega(t)dt = \pi, \quad \phi_1 = \gamma + \pi/2, \quad t \in (5\tau/8, 7\tau/8], \\
&\int_{\frac{7\tau}{8}}^{\tau} \Omega(t)dt = \pi/2, \quad \phi_1 = \gamma + \pi, \quad t \in (7\tau/8, \tau]. \quad (12)
\end{aligned}$$

At the end of the evolution, the evolution operator is given in the computational subspace by $U(\theta, \phi, \gamma) = e^{i\frac{\gamma}{2}}e^{-i\frac{\gamma}{2}\mathbf{n}\cdot\sigma}$ with $\mathbf{n} = (s_\theta c_\phi, s_\theta s_\phi, c_\theta)$ and $\sigma = (\sigma_x, \sigma_y, \sigma_z)$.

The three-qubit gates can be directly realized utilizing the Rydberg blockade mechanism, as shown in Fig. 3. Both the target atom and the control atoms include two ground states $\{|0\rangle, |1\rangle\}$ and one Rydberg excited state $|r\rangle$. The interaction Hamiltonian is $H_I = V_{c1,t}|rr\rangle_{c1,t}\langle rr| + V_{c2,t}|rr\rangle_{c2,t}\langle rr| + V_{c1,c2}|rr\rangle_{c1,c2}\langle rr|$, where the subscripts "$c1(2)$" and "$t$" represent the control atom 1(2) and the target atom, respectively. For simplicity, we set $V_{c1,t} = V_{c2,t} = V_{c1,c2} = V$ denoting the dipole-dipole or van der Waals interaction strength, and $V \gg \Omega$. As long as one of the atoms is excited to the excited state $|r\rangle$, other atoms will not be excited due to the Rydberg blockade mechanism [8,11]. Three-qubit gate operators can be realized by the following three steps:

Step 1: The resonant pulses couple two control atoms successively, in which the Rabi frequency satisfies $\int \Omega_c dt = \pi$.

Step 2: The universal operator $U(\theta, \varphi, \gamma)$ is performed on the target atom, which is realized by the coupled pulses as in Eq. (12). Besides, there are two possible cases: (i) if there is a control atom in the Rydberg state, the target atom cannot perform the desired operation due to the Rydberg blockade mechanism, and thus these states remain unchanged; (ii) the target atom can perform the desired operator if both of the two control atoms are not in the state $|r\rangle$.

Step 3: The reverse operations of Step 1 are performed on the control atoms to deexcite the control atoms from the excited state to ground states, in which we need to inverse the phase of the pulses.

We can obtain our desired three-qubit operator after these steps. In addition, we need to verify the driven pulses

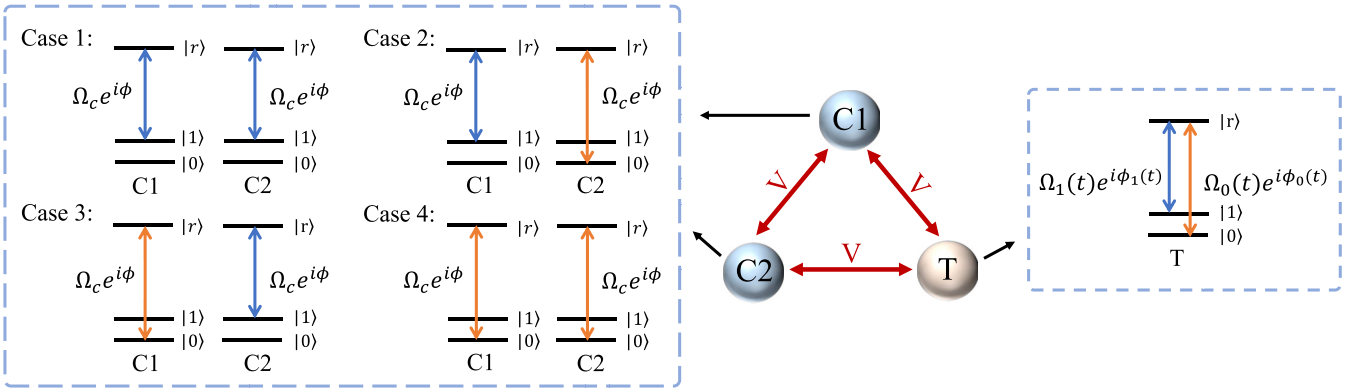

FIG. 3. Illustration of multiqubit gate operators, in which both transitions $|0\rangle \to |r\rangle$ and $|1\rangle \to |r\rangle$ of the control atoms are resonantly driven by $\Omega_c e^{i\phi}$, transitions $|0\rangle \to |r\rangle$ and $|1\rangle \to |r\rangle$ of the target atom are resonantly driven by $\Omega_0(t)e^{i\phi_0(t)}$ and $\Omega_1(t)e^{i\phi_1(t)}$, respectively, and V denotes Rydberg-Rydberg interaction between two atoms.

in the control atoms to obtain our desired gate operators in the realization of the quantum SA, as shown in Fig. 3. For Case 1, we have the three-qubit gate operator $U = |00\rangle_{c1c2}\langle 00| \otimes U_t(\theta,\phi,\gamma) + (I_{c1}I_{c2} - |00\rangle_{c1c2}\langle 00|) \otimes I_t$; for Case 2, we acquire $U = |01\rangle_{c1c2}\langle 01| \otimes U_t(\theta,\phi,\gamma) + (I_{c1}I_{c2} - |01\rangle_{c1c2}\langle 01|) \otimes I_t$; for Case 3, $U = |10\rangle_{c1c2}\langle 10| \otimes U_t(\theta,\phi,\gamma) + (I_{c1}I_{c2} - |10\rangle_{c1c2}\langle 10|) \otimes I_t$; and for Case 4, $U = |11\rangle_{c1c2}\langle 11| \otimes U_t(\theta,\phi,\gamma) + (I_{c1}I_{c2} - |11\rangle_{c1c2}\langle 11|) \otimes I_t$.

B. Realizing three-qubit SA via the geometric control

In the process of realizing one-solution three-qubit SA, the necessary single-qubit gate operators $U_{\pi/4,-\pi/2}$ and $U_{\pi/4,\pi/2}$ can be achieved by the parameter values $\theta = \gamma = \pi/2$, $\phi = -\pi/2$, and $\theta = \phi = \gamma = \pi/2$ according to Sec. III A. For the operator $P_{1.323\pi}(|t_{o1}\rangle)$, the driven pulses of the control atoms are the same as in the Case 1 of the three-qubit gate operator in Sec. III A, and parameters of the target atom are $\theta = 0$, $\phi = 0$, and $\gamma = 1.323\pi$. For the operator $P_{1.323\pi}(|t_{o12}\rangle)$, the driven pulses of control atoms are also the same as in Case 1 and the parameters of the target atom are $\theta = \pi$, $\phi = 0$, and $\gamma = 1.323\pi$. Other gate operators $P_{1.323\pi}(|t_o\rangle)$ used to search the remaining one-solution target states are carried out by changing the driven pulses of the control atoms as in Cases 2–4 of three-qubit operators in Sec. III A and by the parameters of the target atom. For the operator $Q_{1.323\pi}$, the driven pulses of the control atoms are the same as in Case 4, and the parameters of the target atom are set as $\theta = \pi$, $\phi = 0$, and $\gamma = 1.323\pi$. With these operations, all the one-solution target states can be searched with definite success probability.

For two-solution three-qubit SA, the operator $P_\pi(|t_t\rangle)$ is realized by combining two three-qubit gate operators. For example, $P_\pi(|t_{t1}\rangle)$ can be realized by $P_\pi(|t_{t1}\rangle) = U_1U_2$, where $U_1 = |00\rangle_{c1c2}\langle 00| \otimes (e^{i\pi}|0\rangle_t\langle 0| + |1\rangle_t\langle 1|) + (I_{c1}I_{c2} - |00\rangle_{c1c2}\langle 00|) \otimes I_t$ and $U_2 = |00\rangle_{c1c2}\langle 00| \otimes (|0\rangle_t\langle 0| + e^{i\pi}|1\rangle_t\langle 1|) + (I_{c1}I_{c2} - |00\rangle_{c1c2}\langle 00|) \otimes I_t$. The operator $R_\pi(|t_{t2}\rangle)$ is realized by the controlled-phase gates U_1 and U_3, in which $U_3 = |01\rangle_{c1c2}\langle 01| \otimes (e^{i\pi}|0\rangle_t\langle 0| + |1\rangle_t\langle 1|) + (I_{c1}I_{c2} - |01\rangle_{c1c2}\langle 01|) \otimes I_t$, in which the driven pulses of the control atom are realized in Cases 1–4 of three-qubit operators in Sec. III A, and the parameters of the target atom are set as $\theta = \pi, \phi = 0, \gamma = \pi$ or $\theta = 0, \phi = 0, \gamma = \pi$. For the operator Q_π, the driven pulses of the control atoms are the same as in Case 4, and the parameters of the target atom are $\theta = \pi$, $\phi = 0$, and $\gamma = \pi$. These gate operators can be easily obtained in our scheme. Based on the above operations, all two-solution target states can be exactly searched with the QC design in Sec. II C.

IV. PERFORMANCE OF THE THREE-QUBIT SA

To implement the three-qubit SA using the Rb atoms, we choose the relevant energy levels as $|0\rangle = |5S_{1/2}, F = 1, m_F = 0\rangle$, $|1\rangle = |5S_{1/2}, F = 2, m_F = 0\rangle$, and $|r\rangle = |83S, J = m_J = 1/2\rangle$. The two identical atoms are separated by $d = 4$ μm, and the dispersion parameter C_6 of the Rb atom is 9.7×10^3 GHz μm^6. The Rydberg interaction intensity can then be evaluated as $V/2\pi = 2.368$ GHz [1,92]. At the temperature 0 K, the lifetime of the Rydberg state is about $\tau = 696.35\,\mu$s and the decay rate is $\Gamma = 1/\tau$ [9,93]. The frequency of the Rabi oscillations between the ground states and the Rydberg state is $\Omega/2\pi = 10$ MHz, which can be varied by adjusting the waists and optical powers of the lasers as well as the relevant detuning from the intermediate state [94,95].

Taking into account the spontaneous decay of the Rydberg state, we evaluate the performance of the quantum SA by the Lindblad master equation

$$\dot{\rho} = i[\rho, H'] + \frac{\Gamma}{2}\sum_{j=1}^{3}\sum_{i=0}^{1}(2L_j\rho L_j^\dagger - L_j^\dagger L_j\rho - \rho L_j^\dagger L_j), \quad (13)$$

where H' is the total Hamiltonian of the quantum SA, ρ is the density operator of the systematic state, and $L_j = |i\rangle_j\langle r|$ denotes the atomic spontaneous emission from $|r\rangle$ to $|i\rangle$ (j labels the jth atom). We define the fidelity $F = |\langle\psi_{\rm ideal}|\psi\rangle|^2$, where $|\psi_{\rm ideal}\rangle$ denotes the ideal target state and $|\psi\rangle$ denotes the evolved state calculated by numerically solving the master equation.

For the one-solution three-qubit SA, the operator $P_\phi(|t_o\rangle)$ for different target states can be realized directly in our scheme, which avoids some redundant quantum logic operations. To show the advantage of our scheme, we compare

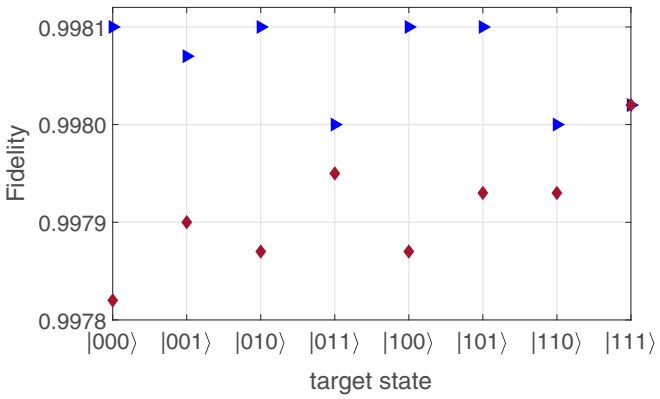

FIG. 4. Fidelity of the three-qubit SA for all one-solution target states, where the blue triangles represent our result and the red diamonds are from a previous work of SA. These two schemes are realized with the same geometric control, in which the decay rate $\Gamma = 1.4$ kHz and the Rabi frequency $\Omega/2\pi = 10$ MHz.

it with the scheme of the previous quantum SA under the same geometric quantum control method. As shown in Fig. 4, we see that our scheme can search the target state with higher fidelity, i.e., at least 99.8%. As a result, the performance of our scheme in realizing the quantum SA is improved compared with the previous scheme.

In addition, the total evolution time of our scheme is reduced, thus the influence of the decoherence can be further suppressed. We have numerically simulated the fidelity as a function of the decay parameter Γ for the one-solution three-qubit SA, as shown in Figs. 5(a) and 5(b), in which the target states are $|t_{o1}\rangle$ and $|t_{o2}\rangle$, respectively. We compare our scheme

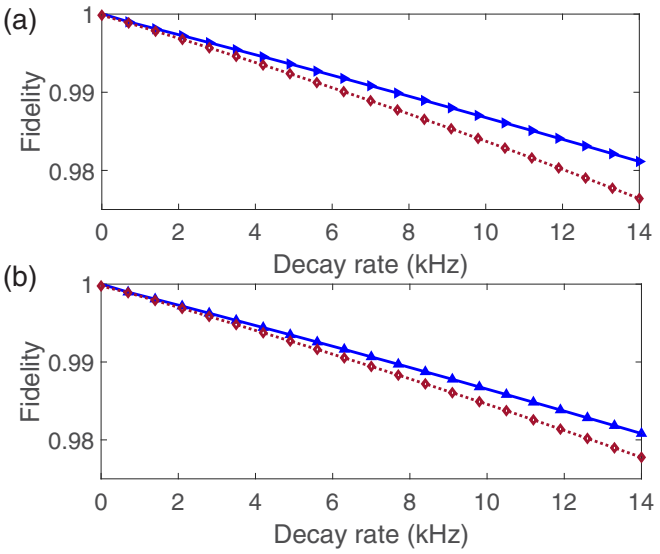

FIG. 5. Fidelity of the three-qubit SA for (a) $|t_{o1}\rangle$ target state and (b) $|t_{o2}\rangle$ target state as functions of the decay rate Γ, where the solid line with blue triangles represents our results, and the dotted line with red diamonds is realized by the QC of a previous SA. These two schemes are realized with the same geometric control, in which the Rabi frequency is $\Omega/2\pi = 10$ MHz.

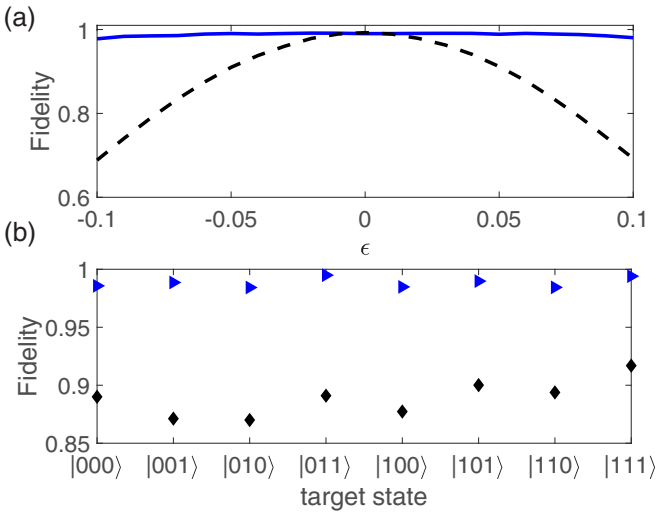

FIG. 6. (a) Numerical results for the robustness to control errors of the three-qubit SA for the one-solution target state $|111\rangle$, where the relative pulse deviation is $\epsilon \in [-0.1, 0.1]$, the blue solid line is the fidelity of the three-qubit SA realized by our scheme, and the black dashed line is realized by conventional geometric control. The QCs of these two schemes are shown in Fig. 3. (b) The fidelity of the three-qubit SA for all one-solution target states, where the relative pulse deviation ϵ is 0.05, the blue triangles represent our scheme, and the black diamonds are the three-qubit SA realized by conventional geometric control. We use the following values: the decay rate $\Gamma = 1.4$ kHz and the Rabi frequency $\Omega/2\pi = 10$ MHz.

with the previous quantum SA scheme, from which we see that our scheme has better robustness against the decoherence.

Finally, the control error is also a crucial factor for realization of quantum algorithms. To show the advantage of our scheme, we first compare the robustness between our scheme and the scheme using conventional geometric control in the search of the target state $|111\rangle$, where the relative pulse deviation ϵ varies in the range $\epsilon \in [-0.1, 0.1]$. As shown in Fig. 6(a), our scheme has great robustness against the control error. To further show the generality of our scheme, we have numerically simulated the fidelity for all the one-solution target states under the existence of the control error, where we assume the relative pulse deviation ϵ to be 0.05, as shown in Fig. 6(b). We find that our scheme has an obvious advantage for suppressing the control error in the realization of the one-solution three-qubit quantum SA.

For the two-solution three-qubit SA, the fidelity dynamics of the system state is depicted in Figs. 7(a) and 7(b), where the target states are $|t_{t1}\rangle$ and $|t_{t2}\rangle$, and we find that target states can be searched with a fidelity of 99.97% and 99.95%, respectively. So our scheme is feasible, and the two-solution three-qubit quantum SA can be realized with high fidelity in the presence of decoherence. In addition, the fidelities as functions of the control error for the quantum SA with two-solution target states $|t_{t1}\rangle$ and $|t_{t2}\rangle$ are presented in Figs. 7(c) and 7(d), from which we see that our scheme can greatly suppress the influence of the systematic error.

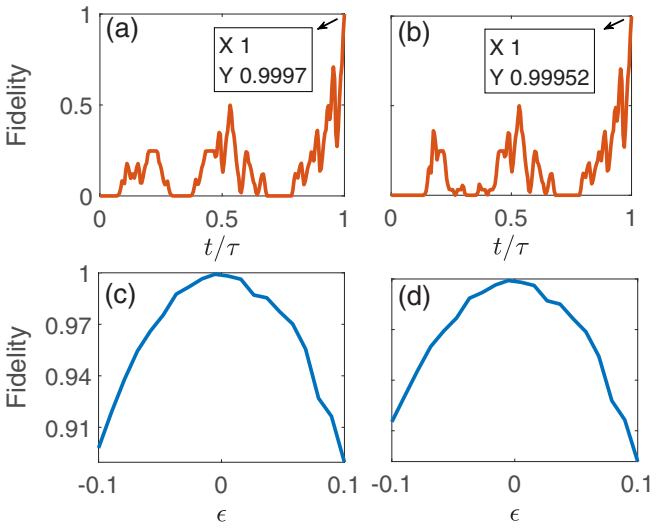

FIG. 7. Fidelity of three-qubit SA varying with time for two-solution target states $|t_{t1}\rangle$ (a) and $|t_{t2}\rangle$ (b), where the total time is $\tau = 3\ \mu$s. Fidelity of three-qubit SA as a function of the control error for two-solution target states $|t_{t1}\rangle$ (c) and $|t_{t2}\rangle$ (d), where the decay rate $\Gamma = 1.4$ kHz and the Rabi frequency $\Omega/2\pi = 10$ MHz.

V. CONCLUSION AND OUTLOOK

In conclusion, we have proposed a scheme to exactly realize a multisolution three-qubit SA, where the number of iterations and phase values can be obtained directly and the corresponding QCs in our scheme are easily designed. This enables us to avoid unwanted complex quantum logic operators. Multiple phase values and fewer logic gate operations may be more helpful for achieving quantum SAs experimentally. We can search the target state with a fidelity of at least 99.8%, and our scheme can better suppress the influence of decoherence. In addition, the numerical simulation results indicate that our scheme can greatly suppress the influence of control errors. Our scheme can also be easily generalized to multisolution multiqubit SAs with definite success probabilities using Rydberg atoms. Finally, we have demonstrated the idea of combining geometric control with a quantum algorithm, which may be of great interest in implementing other quantum algorithms for Rydberg atoms or other quantum platforms.

ACKNOWLEDGMENTS

S.L.S. acknowledges support from National Natural Science Foundation of China (NSFC) under Grant No. 12274376 and a major science and technology project of Henan Province under Grant No. 221100210400. L.L.Y. acknowledges support from National Natural Science Foundation of China (NFSC) under Grant No. 12074346 and Natural Science Foundation of Henan Province (212300410085). M.F. acknowledges support from by Special Project for Research and Development in Key Areas of Guangdong Province under Grant No. 2020B0303300001.

[1] M. Saffman, T. G. Walker, and K. Mølmer, Rev. Mod. Phys. **82**, 2313 (2010).
[2] T. F. Gallagher, *Rydberg Atoms* (Cambridge University Press, Cambridge, UK, 1994).
[3] M. D. Lukin, M. Fleischhauer, R. Cote, L. M. Duan, D. Jaksch, J. I. Cirac, and P. Zoller, Phys. Rev. Lett. **87**, 037901 (2001).
[4] H. Levine, A. Keesling, G. Semeghini, A. Omran, T. T. Wang, S. Ebadi, H. Bernien, M. Greiner, V. Vuletić, H. Pichler, and M. D. Lukin, Phys. Rev. Lett. **123**, 170503 (2019).
[5] M. Saffman and K. Mølmer, Phys. Rev. Lett. **102**, 240502 (2009).
[6] A. E. B. Nielsen and K. Mølmer, Phys. Rev. A **82**, 052326 (2010).
[7] K. Mølmer, L. Isenhower, and M. Saffman, J. Phys. B **44**, 184016 (2011).
[8] E. Urban, T. A. Johnson, T. Henage, L. Isenhower, D. D. Yavuz, T. G. Walker, and M. Saffman, Nat. Phys. **5**, 110 (2009).
[9] L. Isenhower, E. Urban, X. L. Zhang, A. T. Gill, T. Henage, T. A. Johnson, T. G. Walker, and M. Saffman, Phys. Rev. Lett. **104**, 010503 (2010).
[10] T. M. Graham, M. Kwon, B. Grinkemeyer, Z. Marra, X. Jiang, M. T. Lichtman, Y. Sun, M. Ebert, and M. Saffman, Phys. Rev. Lett. **123**, 230501 (2019).
[11] T. Vogt, M. Viteau, A. Chotia, J. Zhao, D. Comparat, and P. Pillet, Phys. Rev. Lett. **99**, 073002 (2007).
[12] S.-L. Su, E. Liang, S. Zhang, J.-J. Wen, L.-L. Sun, Z. Jin, and A.-D. Zhu, Phys. Rev. A **93**, 012306 (2016).
[13] F. M. Gambetta, C. Zhang, M. Hennrich, I. Lesanovsky, and W. Li, Phys. Rev. Lett. **125**, 133602 (2020).
[14] P. P. Mazza, R. Schmidt, and I. Lesanovsky, Phys. Rev. Lett. **125**, 033602 (2020).
[15] S.-L. Su, Y. Gao, E. Liang, and S. Zhang, Phys. Rev. A **95**, 022319 (2017).
[16] D. Petrosyan and K. Mølmer, Phys. Rev. Lett. **113**, 123003 (2014).
[17] C. Ates, T. Pohl, T. Pattard, and J. M. Rost, Phys. Rev. Lett. **98**, 023002 (2007).
[18] S.-L. Su, F.-Q. Guo, J.-L. Wu, Z. Jin, X. Q. Shao, and S. Zhang, Europhys. Lett. **131**, 53001 (2020).
[19] L. Isenhower, M. Saffman, and K. Mølmer, Quant. Inf. Proc. **10**, 755 (2011).
[20] D. Møller, L. B. Madsen, and K. Mølmer, Phys. Rev. Lett. **100**, 170504 (2008).
[21] H.-Z. Wu, Z.-B. Yang, and S.-B. Zheng, Phys. Rev. A **82**, 034307 (2010).
[22] S. L. Su, H. Z. Shen, Erjun Liang, and Shou Zhang, Phys. Rev. A **98**, 032306 (2018).
[23] M. Müller, I. Lesanovsky, H. Weimer, H. P. Büchler, and P. Zoller, Phys. Rev. Lett. **102**, 170502 (2009).
[24] H. Weimer, M. Müller, I. Lesanovsky, P. Zoller, and H. P. Büchler, Nat. Phys. **6**, 382 (2010).

[25] A. Keesling, A. Omran, H. Levine, H. Bernien, H. Pichler, S. Choi, R. Samajdar, S. Schwartz, P. Silvi, S. Sachdev, P. Zoller, M. Endres, M. Greiner, V. Vuletić, and M. D. Lukin, Nature (London) **568**, 207 (2019).

[26] S. Ebadi, T. T. Wang, H. Levine, A. Keesling, G. Semeghini, A. Omran, D. Bluvstein, R. Samajdar, H. Pichler, W. W. Ho, S. Choi, S. Sachdev, M. Greiner, V. Vuletić, and M. D. Lukin, Nature (London) **595**, 227 (2021).

[27] S. Ebadi, A. Keesling, M. Cain, T. T. Wang, H. Levine, D. Bluvstein, G. Semeghini, A. Omran, J.-G. Liu, R. Samajdar, X.-Z. Luo, B. Nash, X. Gao, B. Barak, E. Farhi, S. Sachdev, N. Gemelke, L. Zhou, S. Choi, H. Pichler *et al.*, Science **376**, 1209 (2022).

[28] T. M. Graham, Y. Song, J. Scott, C. Poole, L. Phuttitarn, K. Jooya, P. Eichler, X. Jiang, A. Marra, B. Grinkemeyer, M. Kwon, M. Ebert, J. Cherek, M. T. Lichtman, M. Gillette, J. Gilbert, D. Bowman, T. Ballance, C. Campbell, E. D. Dahl *et al.*, Nature (London) **604**, 457 (2022).

[29] C. Dlaska, K. Ender, G. B. Mbeng, A. Kruckenhauser, W. Lechner, and R. van Bijnen, Phys. Rev. Lett. **128**, 120503 (2022).

[30] D. Deutsch and R. Jozsa, Proc. R. Soc. London A **439**, 553 (1992).

[31] P. W. Shor, SIAM J. Comput. **26**, 1484 (1997).

[32] C. H. Bennett, E. Bernstein, G. Brassard, and U. Vazirani, SIAM J. Comput. **26**, 1510 (1997).

[33] L. K. Grover, Phys. Rev. Lett. **79**, 4709 (1997).

[34] L. K. Grover, Phys. Rev. Lett. **80**, 4329 (1998).

[35] L. K. Grover, Pramana–J. Phys. **56**, 333 (2001).

[36] K. H. Yee, J. Bang, P. M. Alsing, W. A. Miller, and D. Ahn, Quantum Sci. Technol. **5**, 045011 (2020).

[37] V. Gebhart, L. Pezzè, and A. Smerzi, Sci. Rep. **11**, 1288 (2021).

[38] J. Zhang, S. S. Hegde, and D. Suter, Phys. Rev. Lett. **125**, 030501 (2020).

[39] W. Liu, Q. Wu, J. Shen, J. Zhao, M. Zidan, and L. Tong, J. Ambient Intell. Human Comput. **12**, 10425 (2021).

[40] I. L. Chuang, L. M. K. Vandersypen, X. Zhou, D. W. Leung, and S. Lloyd, Nature (London) **393**, 143 (1998).

[41] F. Yamaguchi, P. Milman, M. Brune, J. M. Raimond, and S. Haroche, Phys. Rev. A **66**, 010302(R) (2002).

[42] W. L. Yang, C. Y. Chen, and M. Feng, Phys. Rev. A **76**, 054301 (2007).

[43] M. Hua, M.-J. Tao, and F.-G. Deng, Sci. Rep. **5**, 9274 (2015).

[44] M. Feng, Phys. Rev. A **63**, 052308 (2001).

[45] K.-A. Brickman, P. C. Haljan, P. J. Lee, M. Acton, L. Deslauriers, and C. Monroe, Phys. Rev. A **72**, 050306(R) (2005).

[46] Z. Y. Xu and M. Feng, Phys. Rev. A **78**, 014301 (2008).

[47] W.-L. Yang, H. Wei, F. Zhou, W.-L. Chang, and M. Feng, J. Phys. B **42**, 145503 (2009).

[48] P. G. Kwiat, J. R. Mitchell, P. D. D. Schwindt, and A. G. White, J. Mod. Opt. **47**, 257 (2000).

[49] Z. Diao, Phys. Rev. A **82**, 044301 (2010).

[50] X. D. Wu and G. L. Long, Int. J. Quant. Inf. **05**, 597 (2007).

[51] M. V. Berry, Proc. R. Soc. London A **392**, 45 (1984).

[52] Y. Aharonov and J. Anandan, Phys. Rev. Lett. **58**, 1593 (1987).

[53] P. Solinas, P. Zanardi, and N. Zanghì, Phys. Rev. A **70**, 042316 (2004).

[54] S.-L. Zhu, Z. D. Wang, and P. Zanardi, Phys. Rev. Lett. **94**, 100502 (2005).

[55] S. Filipp, J. Klepp, Y. Hasegawa, C. Plonka-Spehr, U. Schmidt, P. Geltenbort, and H. Rauch, Phys. Rev. Lett. **102**, 030404 (2009).

[56] M. Johansson, E. Sjöqvist, L. M. Andersson, M. Ericsson, B. Hessmo, K. Singh, and D. M. Tong, Phys. Rev. A **86**, 062322 (2012).

[57] S. Berger, M. Pechal, A. A. Abdumalikov, C. Eichler, L. Steffen, A. Fedorov, A. Wallraff, and S. Filipp, Phys. Rev. A **87**, 060303(R) (2013).

[58] F. Wilczek and A. Zee, Phys. Rev. Lett. **52**, 2111 (1984).

[59] J. A. Jones, V. Vedral, A. Ekert, and G. Castagnoli, Nature (London) **403**, 869 (2000).

[60] L.-M. Duan, J. I. Cirac, and P. Zoller, Science **292**, 1695 (2001).

[61] W. Xiang-Bin and M. Keiji, Phys. Rev. Lett. **87**, 097901 (2001).

[62] S.-L. Zhu and Z. D. Wang, Phys. Rev. Lett. **89**, 097902 (2002).

[63] E. Sjöqvist, D. M. Tong, L. M. Andersson, B. Hessmo, M. Johansson, and K. Singh, New J. Phys. **14**, 103035 (2012).

[64] G. F. Xu, J. Zhang, D. M. Tong, E. Sjöqvist, and L. C. Kwek, Phys. Rev. Lett. **109**, 170501 (2012).

[65] S.-L. Zhu and Z. D. Wang, Phys. Rev. A **67**, 022319 (2003).

[66] Y. Ota, Y. Goto, Y. Kondo, and M. Nakahara, Phys. Rev. A **80**, 052311 (2009).

[67] P. Solinas, P. Zanardi, N. Zanghì, and F. Rossi, Phys. Rev. A **67**, 052309 (2003).

[68] Y. Ota and Y. Kondo, Phys. Rev. A **80**, 024302 (2009).

[69] J. T. Thomas, M. Lababidi, and M. Tian, Phys. Rev. A **84**, 042335 (2011).

[70] G. Xu and G. Long, Sci. Rep. **4**, 6814 (2015).

[71] G. Xu and G. Long, Phys. Rev. A **90**, 022323 (2014).

[72] P. Z. Zhao, X.-D. Cui, G. F. Xu, E. Sjöqvist, and D. M. Tong, Phys. Rev. A **96**, 052316 (2017).

[73] T. Chen and Z.-Y. Xue, Phys. Rev. Appl. **10**, 054051 (2018).

[74] G. F. Xu, C. L. Liu, P. Z. Zhao, and D. M. Tong, Phys. Rev. A **92**, 052302 (2015).

[75] P. Z. Zhao, G. F. Xu, Q. M. Ding, E. Sjöqvist, and D. M. Tong, Phys. Rev. A **95**, 062310 (2017).

[76] Z. Zhang, P. Z. Zhao, T. Wang, L. Xiang, Z. Jia, P. Duan, D. M. Tong, Y. Yin, and G. Guo, New J. Phys. **21**, 073024 (2019).

[77] T. H. Xing, X. Wu, and G. F. Xu, Phys. Rev. A **101**, 012306 (2020).

[78] S.-B. Zheng, C.-P. Yang, and F. Nori, Phys. Rev. A **93**, 032313 (2016).

[79] B.-J. Liu, Y.-S. Wang, and M.-H. Yung, Phys. Rev. Res. **3**, L032066 (2021).

[80] S. Li, B.-J. Liu, Z. Ni, L. Zhang, Z.-Y. Xue, J. Li, F. Yan, Y. Chen, S. Liu, M.-H. Yung, Y. Xu, and D. Yu, Phys. Rev. Appl. **16**, 064003 (2021).

[81] S. Li and Z.-Y. Xue, Phys. Rev. Appl. **16**, 044005 (2021).

[82] J. W. Zhang, L.-L. Yan, J. C. Li, G. Y. Ding, J. T. Bu, L. Chen, S.-L. Su, F. Zhou, and M. Feng, Phys. Rev. Lett. **127**, 030502 (2021).

[83] F.-Q. Guo, X.-Y. Zhu, M.-R. Yun, L.-L. Yan, Y. Zhang, Y. Jia, and S.-L. Su, Europhys. Lett. **137**, 55001 (2022).

[84] L. GuiLu, Z. WeiLin, L. YanSong, and N. Li, Commun. Theor. Phys. **32**, 335 (1999).

[85] E. Biham, O. Biham, D. Biron, M. Grassi, D. A. Lidar, and D. Shapira, Phys. Rev. A **63**, 012310 (2000).

[86] D. Li and X. Li, Phys. Lett. A **287**, 304 (2001).
[87] G. L. Long, Phys. Rev. A **64**, 022307 (2001).
[88] M. Waseem, R. Ahmed, M. Irfan, and S. Qamar, Quant. Inf. Proc. **12**, 3649 (2013).
[89] Z. Diao, M. S. Zubairy, and G. Chen, Z. Naturforsch., A **57**, 701 (2002).
[90] M. S. Zubairy, A. B. Matsko, and M. O. Scully, Phys. Rev. A **65**, 043804 (2002).
[91] C. Figgatt, D. Maslov, K. A. Landsman, N. M. Linke, S. Debnath, and C. Monroe, Nat. Commun. **8**, 1918 (2017).
[92] W. Li, D. Viscor, S. Hofferberth, and I. Lesanovsky, Phys. Rev. Lett. **112**, 243601 (2014).
[93] X.-Y. Zhu, Z. Jin, E. Liang, S. Zhang, and S.-L. Su, Ann. Phys. **532**, 2000059 (2020).
[94] T. A. Johnson, E. Urban, T. Henage, L. Isenhower, D. D. Yavuz, T. G. Walker, and M. Saffman, Phys. Rev. Lett. **100**, 113003 (2008).
[95] J. Deiglmayr, M. Reetz-Lamour, T. Amthor, S. Westermann, A. de Oliveira, and M. Weidemüller, Opt. Commun. **264**, 293 (2006).